

A Luminous Yellow Post-AGB Star in the Galactic Globular Cluster M79¹

Howard E. Bond,^{2,3,4} Robin Ciardullo,² and Michael H. Siegel²

Received _____; accepted _____

¹Based in part on observations with the 1.3- and 1.5-m telescopes operated by the SMARTS Consortium at Cerro Tololo Interamerican Observatory.

²Department of Astronomy & Astrophysics, Pennsylvania State University, University Park, PA 16802, USA; heb11@psu.edu

³Space Telescope Science Institute, 3700 San Martin Dr., Baltimore, MD 21218, USA

⁴Visiting astronomer, Cerro Tololo Inter-American Observatory, National Optical Astronomy Observatory, which is operated by the Association of Universities for Research in Astronomy (AURA) under a cooperative agreement with the National Science Foundation.

ABSTRACT

We report discovery of a luminous F-type post-asymptotic-giant-branch (PAGB) star in the Galactic globular cluster (GC) M79 (NGC 1904). At visual apparent and absolute magnitudes of $V = 12.20$ and $M_V = -3.46$, this “yellow” PAGB star is by a small margin the visually brightest star known in any GC. It was identified using CCD observations in the $uBVI$ photometric system, which is optimized to detect stars with large Balmer discontinuities, indicative of very low surface gravities. Follow-up observations with the SMARTS 1.3- and 1.5-m telescopes show that the star is not variable in light or radial velocity, and that its velocity is consistent with cluster membership. Near- and mid-infrared observations with 2MASS and *WISE* show no evidence for circumstellar dust. We argue that a sharp upper limit to the luminosity function exists for yellow PAGB stars in old populations, making them excellent candidates for Population II standard candles, which are four magnitudes brighter than RR Lyrae variables. Their luminosities are consistent with the stars being in a PAGB evolutionary phase, with core masses of $\sim 0.53 M_\odot$.

We also detected four very hot stars lying above the horizontal branch (“AGB-manqué” stars); along with the PAGB star, they are the brightest objects in M79 in the near ultraviolet. In an Appendix, we give periods and light curves for five variables in M79: three RR Lyrae stars, a Type II Cepheid, and a semiregular variable.

Subject headings: stars: AGB and post-AGB — globular clusters: individual (M79)
— distance scale — stars: evolution — stars: variables: RR Lyrae

1. Introduction

The most luminous stars in old populations are expected to be those that have departed from the top of the asymptotic giant branch (AGB) and are evolving to the left in the Hertzsprung-Russell diagram (HRD) at nearly constant luminosity. Around spectral type F, bolometric corrections are smallest, making these “yellow” post-AGB (PAGB) stars the visually brightest members of globular clusters (GCs). The tenth-magnitude F-type star ROA 24 in ω Centauri (also cataloged as HD 116745 and “Fehrenbach’s star”) is the only star in any GC bright enough to be listed in the *Henry Draper Catalogue* (Harding 1965; Dickens & Powell 1973; Gonzalez & Wallerstein 1992). It has often been considered to be a PAGB star—but see our discussion below in §5.3. The Galactic GC NGC 5986 contains two yellow PAGB stars (Alves, Bond, & Onken 2001), likewise the brightest members of their cluster. In the HRD, stars of this rare type lie some four magnitudes above the horizontal branch (HB) and RR Lyrae stars.

Analogous of these objects are known in the field. Two examples are BD +39°4926 (Slettebak, Bahner, & Stock 1961) and HD 46703 (Bond 1970; Luck & Bond 1984). Both are long-period spectroscopic binaries, with orbital periods of 775 days for BD +39°4926 (Kodaira, Greenstein, & Oke 1970) and 600 days for HD 46703 (Hrivnak et al. 2008). There is no published evidence that BD +39°4926 has a variable brightness. However, the cooler HD 46703 lies in a high-luminosity extension of the RR Lyrae pulsational instability strip; it is a semiregular variable with a range of ~ 0.3 mag and a main period of about 29 days (Bond et al. 1984; Hrivnak et al. 2008; Aikawa 2010).

It has been suggested (Bond 1997a,b; see also Vickers et al. 2015) that F- and A-type PAGB stars should be useful Population II standard candles, because on theoretical grounds there should be a sharp upper limit to their luminosity function. Moreover, they are easy to detect using broadband photometry on small telescopes, as their low surface gravities give

them extremely large Balmer jumps. In the late 1990’s, H.E.B. and collaborators began to develop a photometric system optimized for the efficient discovery of such stars. This system combines the u filter of Thuan & Gunn (1976), whose bandpass lies almost entirely shortward of the Balmer jump, with the standard broadband Johnson-Kron-Cousins BVI filters. The design principles of this $uBVI$ system were described by Bond (2005, hereafter Paper I). A network of standard stars was established by Siegel & Bond (2005, hereafter Paper II), based on extensive observations with CCD cameras at 0.9- and 1.5-m telescopes at Kitt Peak National Observatory (KPNO) and Cerro Tololo Interamerican Observatory (CTIO).

In this paper we report our discovery, using $uBVI$ photometry, of a bright PAGB star in the GC M79 (NGC 1904). We then present follow-up photometric and spectroscopic monitoring aimed at placing limits on the variability and binarity of the star. We close with a negative search for circumstellar dust, an argument for the case that Population II PAGB stars are indeed promising standard candles, and a discussion of their evolutionary status. An appendix presents photometry of several known variable stars in M79.

2. $uBVI$ Observations and Discovery of the PAGB Star

As part of our $uBVI$ survey of the Galactic GCs, M79 was imaged on 1997 November 7 with the CTIO 0.9-m telescope and a Tek 2048×2048 CCD detector, giving a field of view of $13'.5 \times 13'.5$. Exposure times in $uBVI$ were 400, 60, 45, and 60 s, respectively. These are relatively shallow frames, aimed at detecting luminous PAGB stars without saturating their images.

The frames were bias-subtracted and flat-fielded using the `CCDPROC` task in IRAF¹, and

¹IRAF is distributed by the National Optical Astronomy Observatory, which is operated

instrumental stellar magnitudes were measured with the DAOPHOT tasks **ALLSTAR** and **DAOGROW** (Stetson 1990). After correction for atmospheric extinction, the photometry was calibrated to the *uBVI* system using observations on the same night of standard-star fields from Paper II.

We show the resulting color-magnitude diagrams (CMDs) of M79 in V vs. $B - V$ in Figure 1a, and in V vs. $V - I$ in Figure 1b. To reduce field-star contamination (which is already quite small), we plot only stars lying within $4'8$ from the cluster center. Because of source confusion, all of the plotted stars are at least $0'5$ from the center. The data have not been corrected for the cluster’s very small reddening of $E(B - V) = 0.01$ (Harris 1996²). Harris gives an M79 distance of 12.9 kpc and a metallicity of $[\text{Fe}/\text{H}] = -1.60$.

CMDs for M79, generally reaching considerably deeper than ours, have been published previously by a number of authors, including Ferraro et al. (1992), Alcaïno et al. (1994), Kravtsov et al. (1997), Rosenberg et al. (2000), Lanzoni et al. (2007), Dalessandro et al. (2012), and Kopacki (2015). These studies used ground-based CCD data and, in the cases of Dalessandro et al. and Lanzoni et al., space-based *Hubble Space Telescope* (*HST*) and *Galaxy Evolution Explorer* (*GALEX*) observations. All of these authors have shown that the cluster has an extremely blue HB with a long blue tail, and a sparsely populated AGB—a CMD that is remarkably similar to that of the better-known M13. Our *BVI* data plotted in Figures 1a and 1b are in complete agreement with these findings.

In Figure 1c we plot the $(u - B) - (B - V)$ color difference vs. $V - I$. The color

by the Association of Universities for Research in Astronomy (AURA) under a cooperative agreement with the National Science Foundation.

²Catalog of Parameters for Milky-Way Globular Clusters, 2010 edition at <http://www.physics.mcmaster.ca/~harris/mwgc.dat>

difference is an analog in the $uBVI$ system of the c_1 index in the Strömgren system; it measures the size of the Balmer jump, while being relatively insensitive to reddening and metallicity (see Paper I for details). The plot shows only stars brighter than $V = 17.75$, and individual stars with errors in either coordinate greater than ± 0.06 mag have been deleted. The distribution of objects peaking on the left-hand side of this figure contains the HB stars, while the sequence of objects on the right-hand side are the subgiants and red giants, plus a small number of AGB stars. The objects clumped around $V - I \simeq 0.65$ are a few foreground field stars.

Five stars stand out in the CMDs and color-color diagrams. Most conspicuous is the very bright PAGB candidate, marked with red filled circles in the three plots; this star is prominent in the $(u - B) - (B - V)$ vs. $V - I$ diagram because of its unusually large Balmer-jump index. Stars with such colors are extremely rare, leaving little doubt that the object is a PAGB star belonging to the cluster. There are also four hot, blue stars lying above the HB, marked with blue filled circles in all three plots in Figure 1. Such objects are usually interpreted as stars evolving off the blue HB, destined to become white dwarfs without ascending the AGB—the so-called AGB-manqué (AGB-M) stars. Table 1 lists properties of these five stars. A finding chart is presented in Figure 2. The two optically faintest AGB-M objects are extremely hot stars, which are very bright in the far- and near-ultraviolet (FUV and NUV, respectively). They had been noted by Hill et al. (1992) in their *Astro-1* Spacelab Ultraviolet Imaging Telescope (UIT) observations of M79, and were designated UIT 1 and UIT 2.

At an absolute magnitude of $M_V = -3.46$ (see below), the M79 PAGB star is by far the visually brightest member of its cluster, and in fact marginally the visually absolutely brightest star known in any GC. To our knowledge, in spite of the many investigations of M79 referenced above, the star had not been recognized previously as belonging to the

cluster. In most studies it goes unmentioned, and has apparently been dismissed as a foreground star; actually, in typical deep CCD exposures, its image would be saturated. The object was, however, designated as star “H” in a photographic study of M79 by Stetson & Harris (1977), who used it as one of their calibration stars; they gave photoelectric measurements of $V = 12.21$, $B - V = 0.30$, and $U - B = 0.24$. Hill et al. (1992) noted its brightness in the NUV—it is the brightest star in their NUV frame—but considered it to be “an early F-type field star” (it being very faint in their FUV image).

Our discovery of the PAGB star in M79 was communicated privately to Şahin & Lambert (2009, hereafter SL09), who obtained high-resolution spectra at McDonald Observatory and carried out an abundance analysis. SL09 reported a very low iron content and a radial velocity (RV) of $+211 \pm 5 \text{ km s}^{-1}$, consistent with the cluster’s RV of $+205.8 \pm 0.4 \text{ km s}^{-1}$ and velocity dispersion of $5.3 \pm 0.4 \text{ km s}^{-1}$ (Harris 1996). Both the low metallicity and the velocity clearly establish the star’s membership in the GC. Their spectroscopic analysis yielded an effective temperature and surface gravity of $T_{\text{eff}} = 6300 \text{ K}$ and $\log g = 0.8$. The very low $\log g$ implied by our $uBVI$ photometry was thus verified. The stellar parameters of the M79 PAGB star are very similar to those of the field PAGB star HD 46703 ($T_{\text{eff}} = 6000 \text{ K}$, $\log g = 0.4$; Luck & Bond 1984). An interesting result of the SL09 analysis was that its iron abundance, $[\text{Fe}/\text{H}] = -2.0$, is about 0.6 dex lower than that of the cluster’s red giants. A similar effect has been seen in field PAGB stars (e.g., Bond 1991), and discussed in terms of depletion of metals onto grains (e.g., Hrivnak et al. 2008 and references therein), but for field stars the progenitor’s original metallicity is considerably less certain.

M79 has been imaged more recently in the NUV with the Ultraviolet Optical Telescope (UVOT) onboard the *Swift* gamma-ray-burst satellite (Siegel et al. 2014). In the UVOT’s *uvw2* bandpass at $\sim 1928 \text{ Å}$, the PAGB star and the four AGB-M stars of our Table 1 are

the five brightest stars in M79 (Siegel et al., their Figure 7).

3. Photometric Monitoring

As noted above, a subset of F-type PAGB stars like HD 46703 are pulsating variables, lying in an extension of the RR Lyrae instability strip. The M79 PAGB star has an effective temperature similar to that of HD 46703 (although both the spectroscopic analyses and optical photometry do imply it to be slightly hotter). We have carried out a program of photometric monitoring to determine whether the M79 star is likewise a pulsating variable.

The observations, made by Chilean service personnel, used the 1.3-m SMARTS Consortium³ telescope at CTIO and its ANDICAM CCD camera. Data were obtained on the M79 PAGB star and surrounding field on 224 nights between 2007 February 20 and 2011 May 8. A typical cadence was every five days, chosen so that a pulsation period of around one month would be easily detected. On each night, two exposures of 30 s each were obtained in B and in V . The usable field of view of these images is about $5'.6 \times 5'.6$.

The ANDICAM frames were bias-subtracted and flat-fielded in the SMARTS pipeline at Yale University. We then carried out photometry on the reduced images. The point-spread function (PSF) of each frame was determined with the DAOPHOT ALLSTAR routine, using 18 bright, isolated stars in the field. The central portion of this PSF (a region slightly larger than the FWHM) was then fit to both the program object and several nearby targets chosen as photometric comparison stars, in order to determine differential magnitudes. Instrumental magnitudes determined in this way were generally precise at a level of ~ 0.005 mag for the PAGB star, and ~ 0.007 mag for typical fainter comparison

³SMARTS is the Small & Moderate Aperture Research Telescope System;
<http://www.astro.yale.edu/smarts>

stars, except for a few frames affected by thick clouds or poor seeing.

For the final analysis, we determined differential magnitudes between the PAGB star and the sum of intensities of eight nearby, constant-brightness comparison stars. Since the PAGB star is bluer than all of the comparison stars (which are a combination of field stars and bright red giants in the cluster), we removed a small mean trend with airmass in the B magnitudes (there was no airmass dependence detected for the V magnitudes).

In Figure 3 we plot the differential magnitudes in B and V , with arbitrary zero points. We see no evidence for variability, certainly not at the level of the ~ 0.3 mag range of HD 46703. There is marginal evidence for slow, low-amplitude variations, particularly during 2009, but these may well be subtle seasonal variations of an instrumental origin.

We also took advantage of this collection of frames for a study of several known variable stars in M79; see Appendix A.

4. Radial-Velocity Monitoring

As noted in the Introduction, several of the known metal-poor A- and F-type PAGB stars in the field are known to be long-period spectroscopic binaries. To investigate whether the M79 PAGB star is also a binary, we monitored its RV on 67 nights over the interval from 2007 February 21 to 2012 January 29. The queue-scheduled spectroscopic observations were made by Chilean service observers with the SMARTS 1.5-m telescope at CTIO, using the RC-focus spectrograph equipped with a CCD camera. Two different setups were employed with grating number 47: setting “47/II,” covering 3878–4552 Å, was used primarily during the first half of the observing interval; during the second half, setting “47/IIb,” covering 4070–4744 Å, was used for most of the observations. Both setups yielded a spectral resolution of 1.6 Å. Exposure times each night were generally 3×300 s, and

short exposures of a HeAr calibration lamp were taken before and after each set of stellar observations.

The CCD images were bias-subtracted and flat-fielded, combined for cosmic-ray removal, and then the stellar spectrum was extracted and wavelength-calibrated, all using standard IRAF routines. In Figure 4, we show a spectrum created by combining all of the data, and normalizing to a flat continuum. The spectrum is dominated by sharp, strong lines of the Balmer series and Ca II H and K. All other lines are relatively quite weak.

On about half of the nights, an RV standard star was observed with the same grating setup. The standard stars we used were 6 Ceti (2 spectra with 47/II, 1 with 47/IIb), 5 Serpentis (2 spectra with 47/IIb), 10 Tauri (4 spectra with 47/II, 15 with 47/IIb), and β Virginis (2 spectra with 47/II, 6 with 47/IIb). We adopted the absolute RVs for these stars given by Stefanik, Latham, & Torres (1999).

We used the IRAF task `fxcor`, which determines RVs (including corrections to the heliocentric frame) through cross-correlation of the program spectrum with a spectrum of a star of known RV. We employed a two-stage process. First, each individual spectrum of the M79 star was cross-correlated with each of the standard-star spectra taken with the same setup, and for each PAGB spectrum we adopted the mean of these determinations. Because the Ca II H and K features in the standard stars are much stronger and broader than in the PAGB star, and because the metallic lines are so weak in the PAGB star, we only used small 40 Å-wide wavelength windows around H δ and H γ for this first pass. The mean RV of the PAGB star was found to be +218.5 km s⁻¹ for the 47/II observations, and +207.0 km s⁻¹ for 47/IIb, with standard deviations of 5.0 and 7.5 km s⁻¹, respectively.

The spectra of the PAGB star and the standard stars, which are F-type subgiants and dwarfs with much higher metallicities and gravities, are not very well matched. Therefore, in a second pass, we cross-correlated each individual PAGB spectrum with the ensemble of

all PAGB spectra taken with the same setup, setting the standard velocity of each spectrum in the ensemble to the mean velocity from the first pass, $+212.9 \text{ km s}^{-1}$. In the second pass, the entire spectral wavelength range was used in the correlations. This resulted in mean RVs of $+213.1 \text{ km s}^{-1}$ for the 47/II spectra, and $+213.4 \text{ km s}^{-1}$ for the 47/IIb spectra, with standard deviations of 4.7 and 5.5 km s^{-1} , respectively.

Figure 5 plots our final velocities versus time. There is no evidence for variations in excess of the errors. The peak-to-peak RV variations for BD +39°4926 and HD 46703 are ~ 30 and $\sim 34 \text{ km s}^{-1}$, respectively (Kodaira, Greenstein, & Oke 1970; Hrivnak et al. 2008). Velocity variations of this size are definitely ruled out for the M79 PAGB star, but, given the modest precision of our measurements, we cannot exclude a binary with a low RV amplitude, or one viewed close to pole-on.

5. Discussion

5.1. No Evidence for Circumstellar Dust

Substantial circumstellar (CS) dust is a well-known feature of PAGB stars belonging to Galactic-disk populations (see the review by van Winckel 2003, and references therein). To search for CS dust around the M79 PAGB star, we determined its spectral-energy distribution (SED) by combining our optical photometry (Table 1) with the *Swift* UVOT measurements by Siegel et al. (2014), and near- and mid-IR photometry from 2MASS (Skrutskie et al. 2006) and *WISE* (Wright et al. 2010). These data points are plotted in Figure 6. Also shown is a blackbody spectrum for $T_{\text{eff}} = 6300 \text{ K}$, which is the effective temperature of the M79 star determined in the spectroscopic analysis by SL09.

As the figure illustrates, the blackbody curve fits the SED extremely well. There is no evidence for CS dust out to a wavelength of $12 \mu\text{m}$, and the star was not detected by *WISE*

at $22\,\mu\text{m}$. The lack of dust may plausibly be explained in part by the star’s low metallicity, making dust formation difficult in the first place; however, the photospheric iron depletion, mentioned in §2, may require that there was some dust formation in the past. In any case, the long post-AGB evolutionary timescales for low-mass remnants in old stellar populations may allow sufficient time for any CS dust that was formed to have dissipated. Note also that near- or mid-IR excesses have not been detected in the field analogs BD +39°4926 and HD 46703.

A further conclusion is that the M79 PAGB star will not produce a planetary nebula (PN). It has been argued that the few PNe known in Milky Way and Local Group GCs are descended from binary-star interactions, and not from single stars (e.g., Jacoby et al. 2013; Bond 2015; and references therein).

5.2. F- and A-Type PAGB Stars as Standard Candles

As mentioned in §1, it has been proposed that yellow PAGB stars in old populations are promising standard candles. In Table 2, we assemble V -band photometry for four such candidates known in GCs: ROA 24 in ω Cen, the two in NGC 5986, and the M79 star discussed in this paper. We calculated visual absolute magnitudes, using the visual apparent distance moduli from the sources cited in the table.

ROA 24 deserves some discussion. It has traditionally been considered to be a PAGB star, along with the visually second-brightest star in ω Cen, the RV Tauri-type variable V1 (e.g., Gonzalez & Wallerstein 1994; van Loon et al. 2007; McDonald et al. 2011). However, the bolometric luminosities of both stars are below that of the AGB tip in ω Cen (for example, McDonald et al. 2009, their Fig. 3; McDonald et al. 2011, their Fig. 1). This suggests that ROA 24 and V1 may more properly be regarded as post-early-AGB stars

(e.g., Dorman et al. 1993, their Fig. 1), rather than stars evolving off the tip of the AGB. In our Table 2, the absolute magnitude of ROA 24 is indeed ~ 0.2 – 0.3 mag fainter than for the other three PAGB candidates.

Setting aside ROA 24, we find a mean visual absolute magnitude for the remaining three stars in Table 2 of $M_{V,0} = -3.38$, with a standard deviation of 0.09 mag, and an error of the mean of only 0.05 mag.

This scatter is considerably smaller than the cosmic scatter in the period-luminosity relation for Cepheid variables. There is no evidence for variability or circumstellar dust for any of the stars, strengthening the case that they are well-behaved candidates for standard candles. They are intrinsically four magnitudes brighter than RR Lyrae stars, and as bright as Cepheids with periods of about 5.3 days. Moreover, unlike RR Lyrae stars and Cepheids, PAGB stars do not require a long series of photometric observations for their discovery: the total exposure time, with a 0.9-m telescope, needed to discover the M79 star was less than 10 minutes. They are expected to be present in old populations that do not contain Cepheids, including elliptical galaxies and dwarf spheroidals. And these objects should exist in halos of spiral galaxies, where there are fewer complications due to interstellar extinction than encountered for Population I Cepheids in the disks.

A practical difficulty is the existence of fainter, but still very low-gravity, stars like ROA 24 and V1 in ω Cen. For PAGB stars to be a robust distance indicator, it will be necessary to sample a large enough population to assure that the upper edge of the luminosity function has been detected.

In subsequent papers, we will report searches for additional PAGB stars in GCs and in the halo of M31. In the next few years, we expect that parallaxes from *Gaia* will provide an excellent zero-point calibration, based on PAGB stars in the field, as well as in Galactic GCs.

5.3. Evolutionary Status

For a mean $M_V = -3.38$, and neglecting the small difference in bolometric corrections between them and the Sun ($M_V = +4.86$), the PAGB candidates in NGC 5986 and M79 have an average luminosity of $\log L/L_\odot \simeq 3.30$. Using the theoretical core-mass/luminosity relation for PAGB stars of Vassiliadis & Wood (1994), $L/L_\odot = 56694(M/M_\odot - 0.5)$, we find a core mass of $\sim 0.53 M_\odot$. This is in excellent agreement with the masses inferred for white dwarfs in GCs (e.g., Kalirai et al. 2009 found $0.53 \pm 0.01 M_\odot$ for the white dwarfs in four Galactic GCs). Thus the case is strengthened that these three stars are in their final PAGB evolutionary stages, just before arriving at the top of the white-dwarf cooling sequence. However, we cannot entirely rule out more complicated scenarios such as those involving binary interactions. Complete surveys for these objects in the Galactic GC system, and in the halos of nearby spirals, would provide information on the lifetimes of the F- and A-type PAGB stars, and thus shed more light on their evolutionary status.

We thank the STScI Director’s Discretionary Research Fund for supporting our participation in the SMARTS consortium, Fred Walter for scheduling the 1.5-m queue observations, and Phil Massey for advice on the use of `fxcor`. We especially appreciate the excellent work of the CTIO/SMARTS service observers who obtained the direct images and spectra during many long clear Tololo nights: Claudio Aguilera, Edgardo Cosgrove, Juan Espinoza, Manuel Hernández, Rodrigo Hernández, Alberto Miranda, Alberto Pasten, Jacqueline Seron, John Subasavage, Joselino Vasquez, and José Velásquez. This publication makes use of data products from the Two Micron All Sky Survey, which is a joint project of the University of Massachusetts and the Infrared Processing and Analysis Center/California Institute of Technology, funded by the National Aeronautics and Space Administration and the National Science Foundation. It also makes use of data products from the Wide-field Infrared Survey Explorer, which is a joint project of the University of California, Los

Angeles, and the Jet Propulsion Laboratory/California Institute of Technology, funded by the National Aeronautics and Space Administration.

Facilities: CTIO:0.9-m, CTIO:1.3m, CTIO:1.5m

A. Variable Stars in M79

The population of variable stars in M79 has been studied by several authors, including Rosino (1952), Amigo et al. (2011), Kains et al. (2012), and Kopacki (2015). In our photometric monitoring with the SMARTS 1.3-m telescope, described in §3, the relatively small field was centered on the PAGB star and thus covered only a portion of the cluster. Nevertheless, one candidate Population II Cepheid, a red giant of uncertain variable type, and three RR Lyrae variables are contained in our field, so we were able to obtain data on them over five observing seasons between 2007 and 2011. Table 3 lists these variables and the elements (zero phase and period) used to prepare the phased light curves given below. The designations are those of the online catalog of variables in GCs maintained by C. Clement⁴. We did not attempt photometry of several low-amplitude variable red giants and SX Phe stars identified by Kopacki (2015), nor of variables in the crowded central regions of the cluster.

Figure 7 shows the nominal locations of the five variables in the cluster’s CMD. The photometric measures were reduced as described in §3, i.e., we determined differential magnitudes between each variable and the intensity sum of eight constant stars in the field. For purposes of plotting light curves, the magnitude zero points were set to arbitrary values. Details of the results are as follows.

⁴Version of 2013 July at <http://www.astro.utoronto.ca/~cclement/cat/listngc.html>

V6: This RRc variable was discovered by Rosino (1952), and extensive data have been obtained by Amigo et al. (2011), Kains et al. (2012), and Kopacki (2015). The modern authors have commented that the period appears to be variable, and we have confirmed this: it proved impossible to fit a single period to all of our data. By breaking our data into five individual annual seasons, and finding periods with a Lafler-Kinman (1965) periodogram, we did find that each season’s data could be fitted reasonably well with a single period. However, the period changes from season to season. By making slight adjustments in the epochs of zero phase, it was possible to superpose all of the seasonal light curves. Table 4 summarizes the elements used for this superposition. Figure 8 shows the resulting light curves, with color coding to indicate the individual seasons. The light curve shape is remarkably constant over our observing interval; only the period and zero-point appear to change. We investigated whether this might be due to a light-travel-time effect in a binary system, but could not find convincing evidence for such an interpretation. The variable period appears instead to be a Blazhko effect.

V7 and V8: These two variables were discovered by Chu (1974)⁵, but little was known about them until quite recently. V7 was classified as a W Virginis-type Population II Cepheid by Kopacki (2015) with a period of 13.985 days, although this was based on only a few cycles of pulsation. Our 2007–2011 data confirm V7 as a W Vir variable, with a best-fit period of 13.9995 days. Figure 9 (top panel) plots its phased light curve.

To the best of our knowledge, there is no previously published light curve for V8; thus its classification has remained unclear, apart from the fact that it lies near the tip of the red-giant branch in the HRD. Our light curve, shown in Figure 9 (bottom panel), shows that it is a semiregular variable, with characteristic alternating depths of minima.

⁵We thank Profs. You-Hua Chu (no relation) and Yang Chen for obtaining a digital scan of this paper and providing an English summary.

Periodograms for the individual annual seasons give periods ranging from 65.1 to 80.1 days; for the entire data set, the analysis gives an average period of about 70.4 days. Several similar variables are known, for example, in M13 (e.g., Osborn & Fuenmayor 1977; Kopacki et al. 2003)—which, as noted in §2, has a very similar CMD to that of M79.

V13 and V14: V13 is an RRab variable, discovered by Amigo et al. (2011), who give a period of 0.6906617 days. Kains et al. (2012) found a period of 0.689391 days. Our data from 2007 to 2011 are best fit with a very similar period of 0.689399 days, as shown in the phased light curves in Figure 10 (top panel). There is significant crowding at the location of V13, and it is located near the edge of the 1.3m- field, making our data unusually noisy.

V14 is an RRc type variable that was discovered by Kains et al. (2012). Our data confirm their period of 0.323733 days, as shown in Figure 10 (bottom panel).

The data for the five variable stars are included in this paper as a machine-readable table. Table 5 illustrates the format of the table.

REFERENCES

- Aikawa, T. 2010, *A&A*, 514, A45
- Alcaino, G., Liller, W., Alvarado, F., & Wenderoth, E. 1994, *AJ*, 107, 230
- Alves, D. R., Bond, H. E., & Onken, C. 2001, *AJ*, 121, 318
- Amigo, P., Catelan, M., Stetson, P. B., et al. 2011, in *RR Lyrae Stars, Metal-Poor Stars, and the Galaxy*, ed. A. McWilliam (Pasadena: Carnegie Institution), 127
- Bond, H. E. 1970, *ApJS*, 22, 117
- Bond, H. E. 1991, in *IAU Symp. 145, Evolution of Stars: the Photospheric Abundance Connection*, eds. G. Michaud & A. Tutukov (Dordrecht: Kluwer), 341
- Bond, H. E. 1997a, in *The Extragalactic Distance Scale*, ed. M. Livio, M. Donahue, & N. Panagia (Cambridge: Cambridge Univ. Press), 224
- Bond, H. E. 1997b, in *Planetary Nebulae*, *IAU Symp. 180*, ed. H. J. Habing & H. J. G. L. M. Lamers (Dordrecht: Kluwer), 460
- Bond, H. E. 2005, *AJ*, 129, 2914 (Paper I)
- Bond, H. E. 2015, *AJ*, 149, 132
- Bond, H. E., Carney, B. W., & Grauer, A. D. 1984, *PASP*, 96, 176
- Chu, Y. 1974, *Acta Astronomica Sinica*, 15, 98
- Dallessandro, E., Salaris, M., Ferraro, F. R., Mucciarelli, A., & Cassisi, S. 2013, *MNRAS*, 430, 459
- Dickens, R. J., & Powell, A. L. T. 1973, *MNRAS*, 161, 249
- Dorman, B., Rood, R. T., & O’Connell, R. W. 1993, *ApJ*, 419, 596
- Ferraro, F. R., Clementini, G., Fusi Pecci, F., Sortino, R., & Buonanno, R. 1992, *MNRAS*, 256, 391

- Gonzalez, G., & Wallerstein, G. 1992, MNRAS, 254, 343
- Gonzalez, G., & Wallerstein, G. 1994, AJ, 108, 1325
- Harding, G. A. 1965, Royal Greenwich Observatory Bulletins, 99, 65
- Harris, W.E. 1996, AJ, 112, 1487
- Hill, R. S., Hill, J. K., Landsman, W. B., et al. 1992, ApJ, 395, L17
- Hrivnak, B. J., Van Winckel, H., Reyniers, M., et al. 2008, AJ, 136, 1557
- Jacoby, G. H., Ciardullo, R., De Marco, O., et al. 2013, ApJ, 769, 10
- Kains, N., Bramich, D. M., Figuera Jaimes, R., et al. 2012, A&A, 548, A92
- Kalirai, J. S., Saul Davis, D., Richer, H. B., et al. 2009, ApJ, 705, 408
- Kodaira, K., Greenstein, J. L., & Oke, J. B. 1970, ApJ, 159, 485
- Kopacki, G. 2015, Acta Astron., 65, 81
- Kopacki, G., Kołaczkowski, Z., & Pigulski, A. 2003, A&A, 398, 541
- Kravtsov, V., Ipatov, A., Samus, N., et al. 1997, A&AS, 125, 1
- Laflier, J., & Kinman, T. D. 1965, ApJS, 11, 216
- Lanzoni, B., Sanna, N., Ferraro, F. R., et al. 2007, ApJ, 663, 1040
- Luck, R. E., & Bond, H. E. 1984, ApJ, 279, 729
- Matsunaga, N., Fukushi, H., Nakada, Y., et al. 2006, MNRAS, 370, 1979
- McDonald, I., van Loon, J. T., Decin, L., et al. 2009, MNRAS, 394, 831
- McDonald, I., van Loon, J. T., Sloan, G. C., et al. 2011, MNRAS, 417, 20
- Osborn, W., & Fuenmayor, F. 1977, AJ, 82, 395
- Rosenberg, A., Piotto, G., Saviane, I., & Aparicio, A. 2000, A&AS, 144, 5
- Rosino, L. 1952, Mem. Soc. Astron. Italiana, 23, 101

- Şahin, T., & Lambert, D. L. 2009, MNRAS, 398, 1730 (SL09)
- Siegel, M. H., & Bond, H. E. 2005, AJ, 129, 2924 (Paper II)
- Siegel, M. H., Porterfield, B. L., Linevsky, J. S., et al. 2014, AJ, 148, 131
- Skrutskie, M. F., Cutri, R. M., Stiening, R., et al. 2006, AJ, 131, 1163
- Slettebak, A., Bahner, K., & Stock, J. 1961, ApJ, 134, 195
- Stefanik, R. P., Latham, D. W., & Torres, G. 1999, in IAU Colloq. 170: Precise Stellar Radial Velocities, eds. J. Hearnshaw & C. Scarfe (San Francisco: ASP), 354
- Stetson, P. B. 1990, PASP, 102, 932
- Stetson, P. B., & Harris, W. E. 1977, AJ, 82, 954
- Thuan, T. X., & Gunn, J. E. 1976, PASP, 88, 543
- van Leeuwen, F., Le Poole, R. S., Reijns, R. A., Freeman, K. C., & de Zeeuw, P. T. 2000, A&A, 360, 472
- van Loon, J. T., van Leeuwen, F., Smalley, B., et al. 2007, MNRAS, 382, 1353
- van Winckel, H. 2003, ARA&A, 41, 391
- Vassiliadis, E., & Wood, P. R. 1994, ApJS, 92, 125
- Vickers, S. B., Frew, D. J., Parker, Q. A., & Bojičić, I. S. 2015, MNRAS, 447, 1673
- Wright, E. L., Eisenhardt, P. R. M., Mainzer, A. K., et al. 2010, AJ, 140, 1868

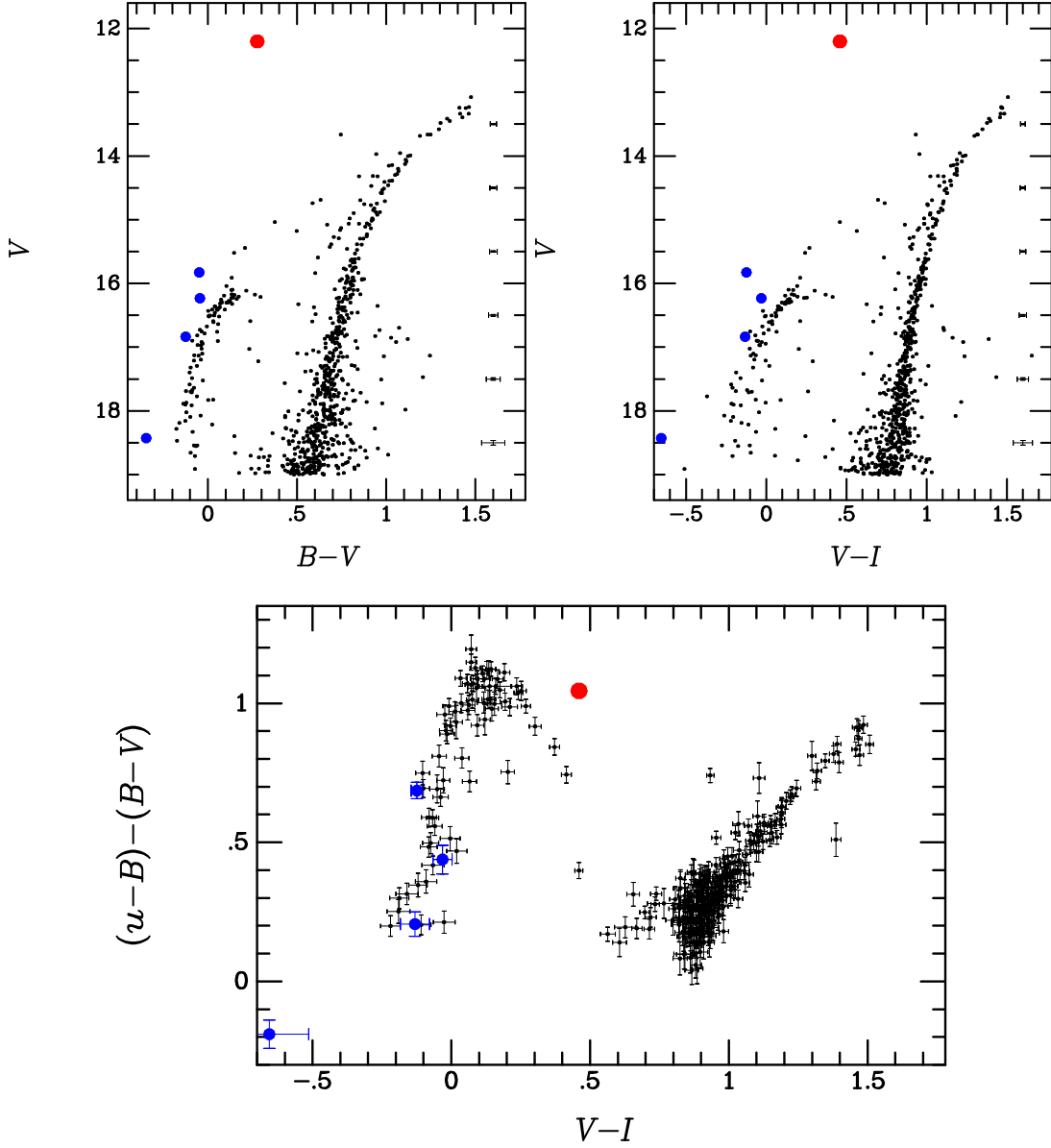


Fig. 1.— (a and b): Color-magnitude diagrams for M79 in $V, B-V$ and $V, V-I$. Stars lying within $4/8$ of the cluster center are plotted. Average photometric error bars as a function of V magnitude are plotted on the right-hand sides. The *filled red circle* shows the location of the luminous PAGB star. Four AGB-manqué stars evolving off the horizontal branch are shown as *filled blue circles*. (c): The gravity-sensitive $(u-B)-(B-V)$ color index plotted against the temperature-sensitive $V-I$ color, for stars brighter than $V = 17.75$. The sequence peaking on the left-hand side of the diagram is the horizontal branch. The sequence on the right-hand side is the subgiant and red-giant branch. The PAGB star stands out because of its low $\log g$ and very large Balmer jump. (The small clump at about $V-I \simeq 0.65$ is foreground field stars.)

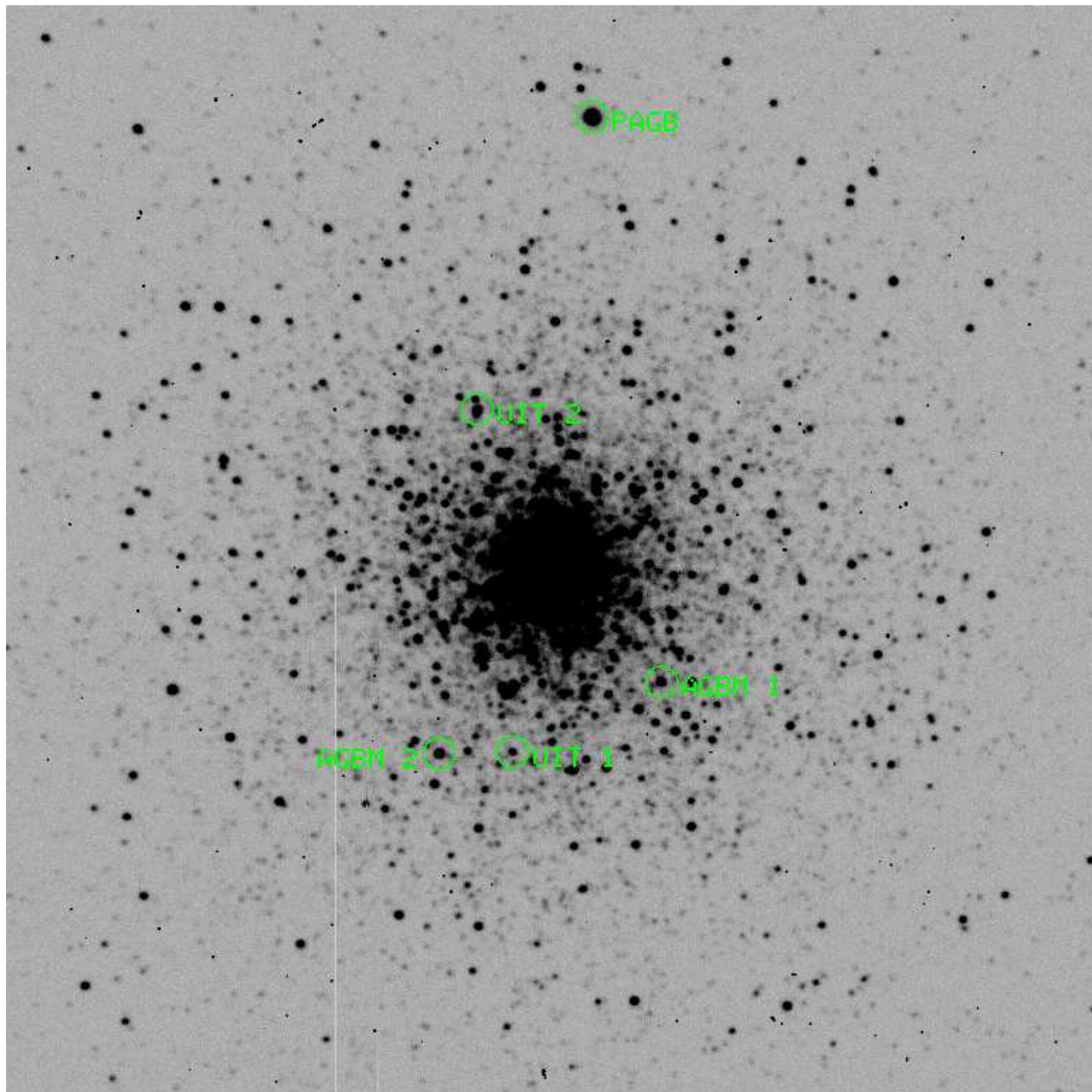


Fig. 2.— Finding chart for the PAGB and AGB-manqué stars in M79 listed in Table 1, made from our 400-s *u*-band exposure with the CTIO 0.9-m telescope. The field is $5'.0 \times 5'.0$ and has north at the top, east on the left. UIT 2 is blended with a close, cooler star.

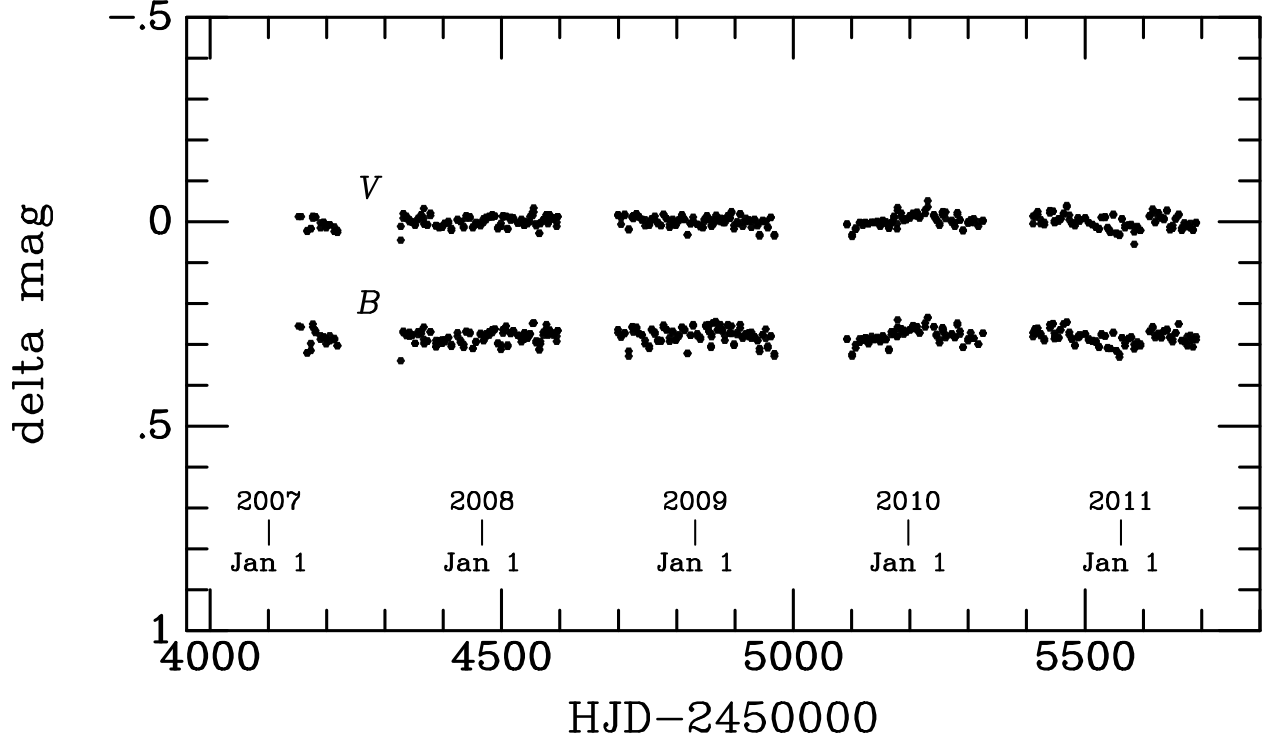


Fig. 3.— Differential photometry for the M79 PAGB star from early 2007 to mid-2011, derived from observations with the SMARTS 1.3-m telescope and CCD camera. We plot the magnitude difference between the PAGB star and the intensity sum of eight nearby comparison stars, with arbitrary zero points. The star appears to be constant within the errors.

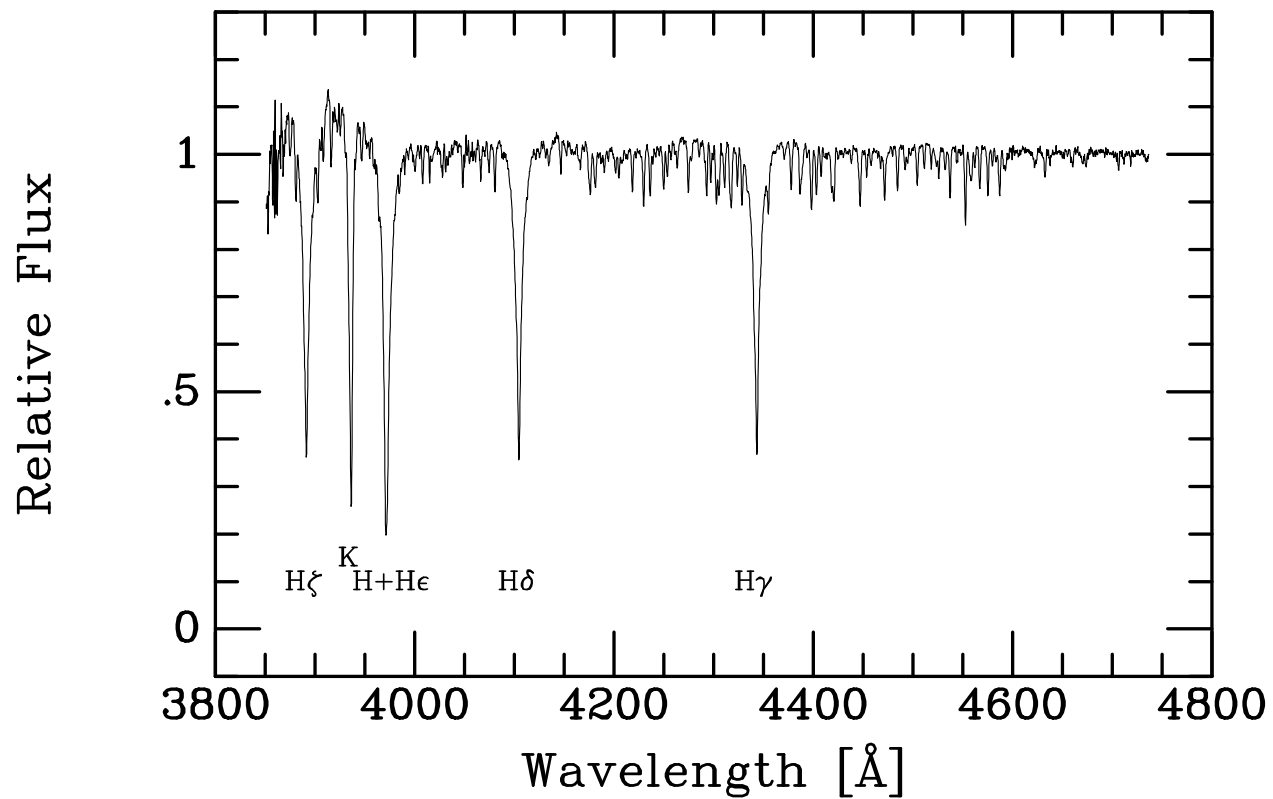


Fig. 4.— Mean spectrum of the M79 PAGB star (resolution ~ 1.6 Å), created by combining data from 67 individual observations made with the SMARTS 1.5-m RC spectrograph, and normalizing to a flat continuum.

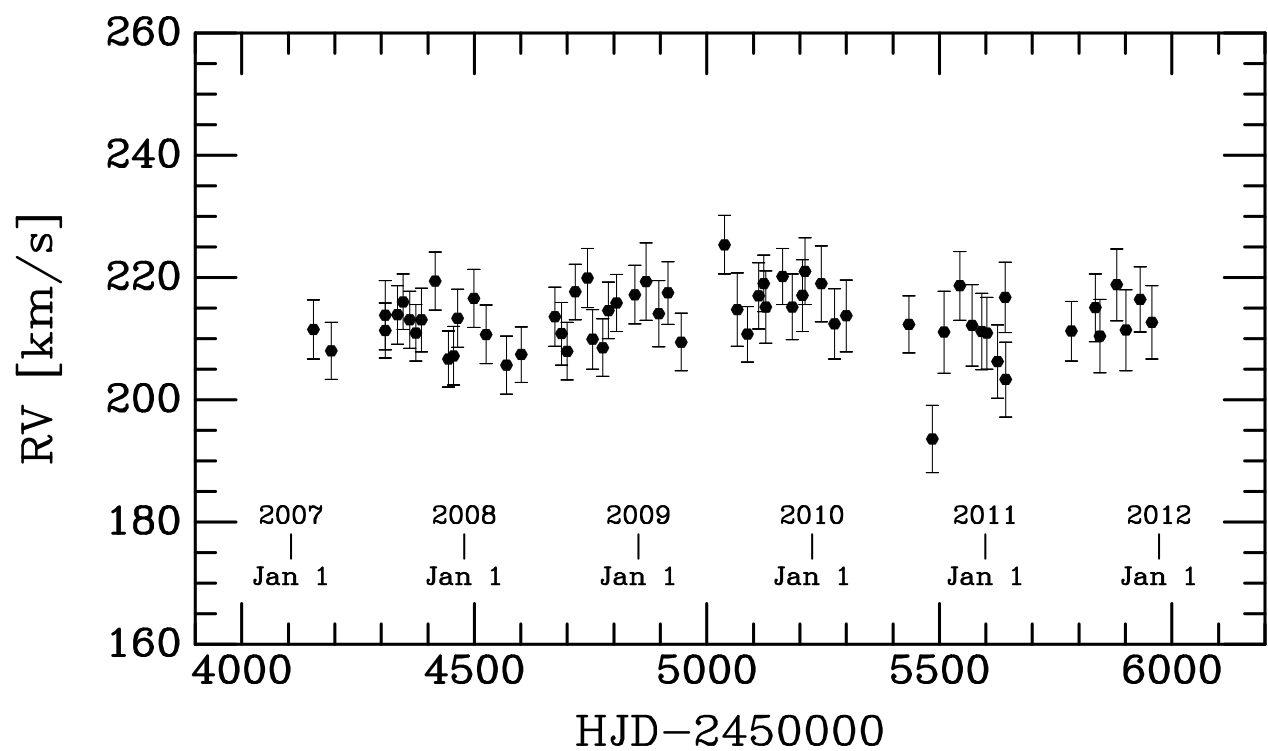


Fig. 5.— Radial-velocity measurements of the M79 PAGB star, based on observations made with the SMARTS 1.5-m RC spectrograph. Within the errors, there is no evidence for velocity variability.

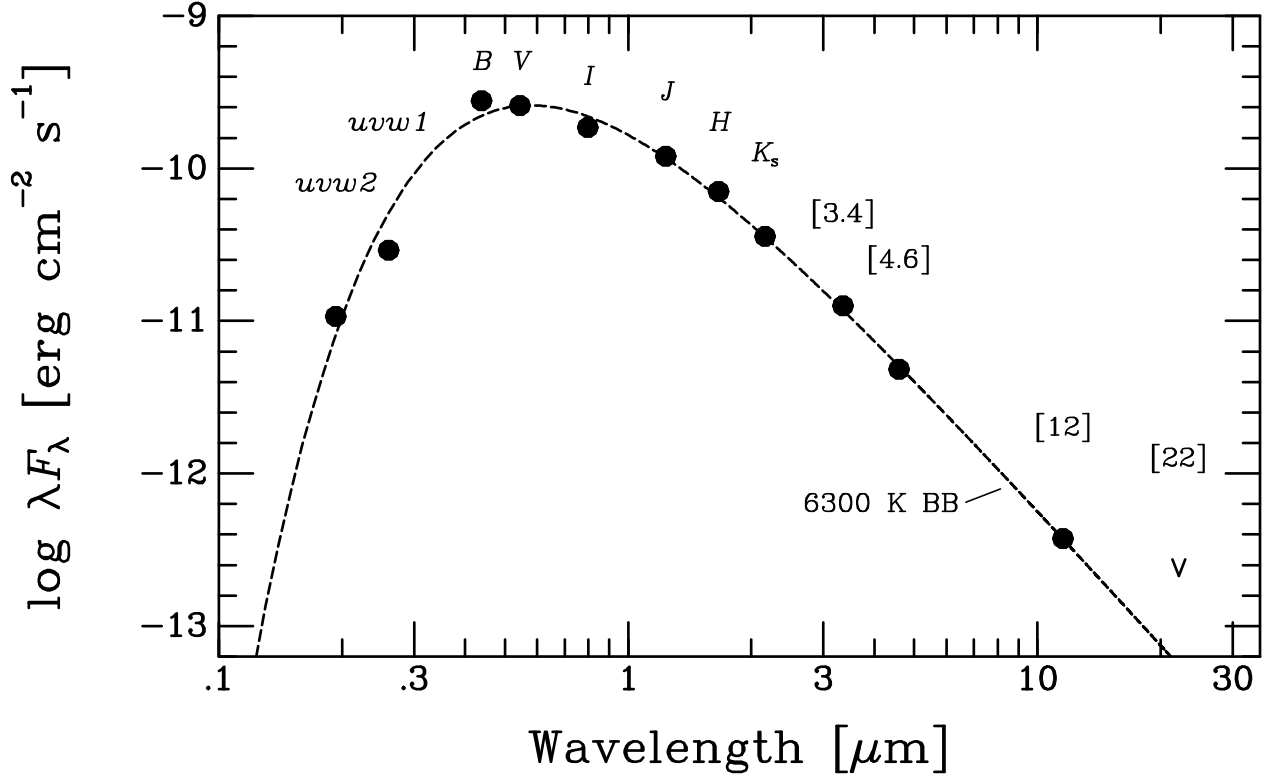


Fig. 6.— The SED of the M79 PAGB star, based on photometry by the *Swift* UVOT, our ground-based photometry from Table 1, and the 2MASS and *WISE* surveys. The point at 22 μm is an upper limit. See text for details. Also shown is a blackbody spectrum for $T_{\text{eff}} = 6300$ K, the temperature obtained in a spectroscopic analysis of the star, normalized to the *V* magnitude. There is no evidence in the near- or mid-IR for circumstellar dust.

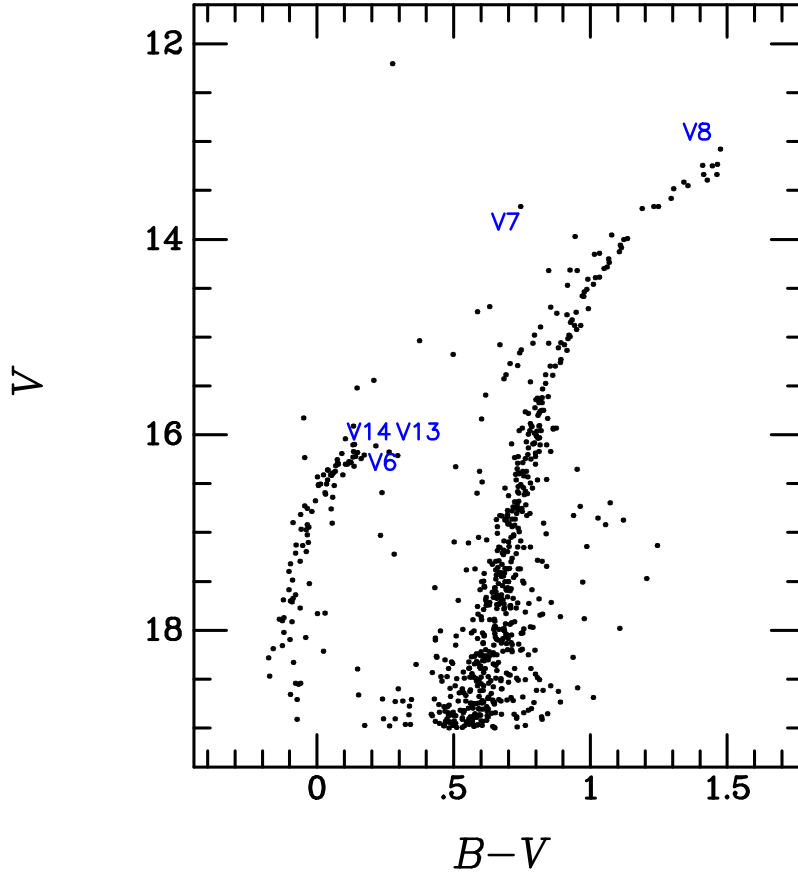


Fig. 7.— Color-magnitude diagram of M79 (taken from Figure 1a), with nominal locations of five variable stars indicated by their designations.

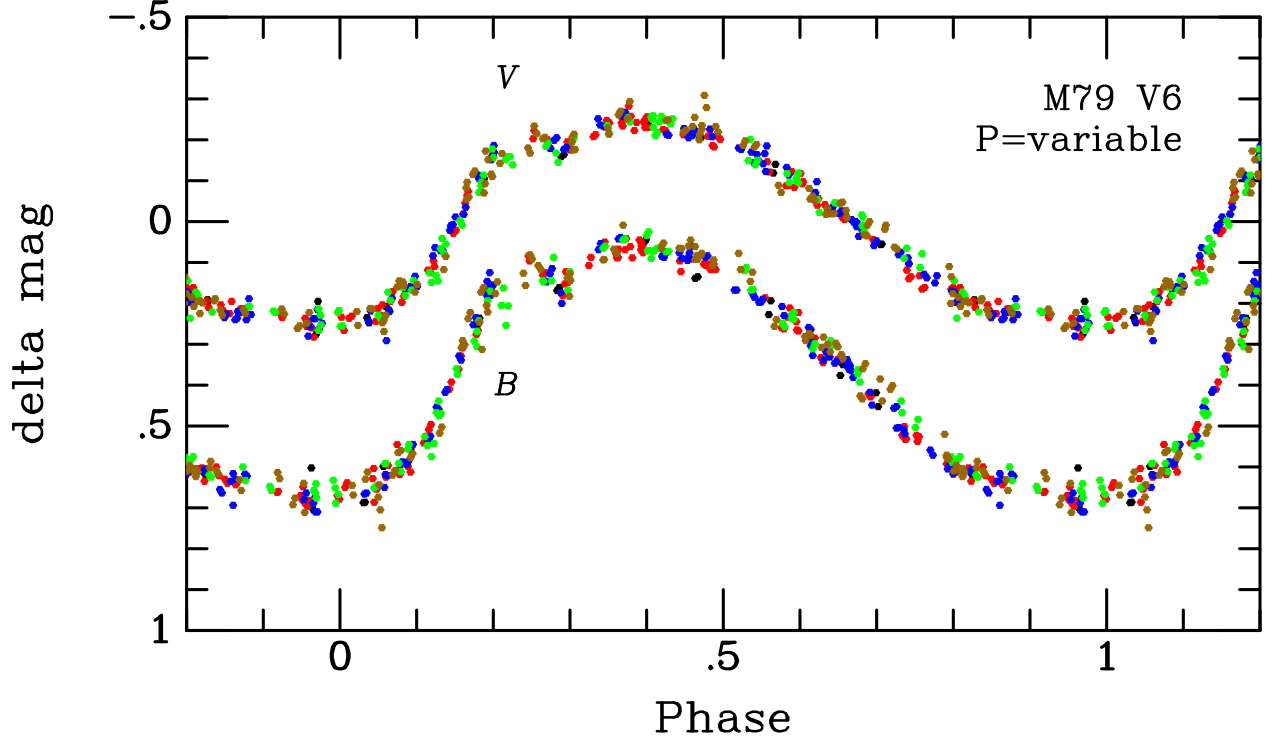


Fig. 8.— Light curves of the RRc variable M79-V6 in V and B , phased according to the seasonal elements given in Table 4. Color coding is: black (2007), red (2007-2008), blue (2008-2009), green (2009-2010), and brown (2010-2011). The light-curve shape appears constant, but the phases and periods are variable.

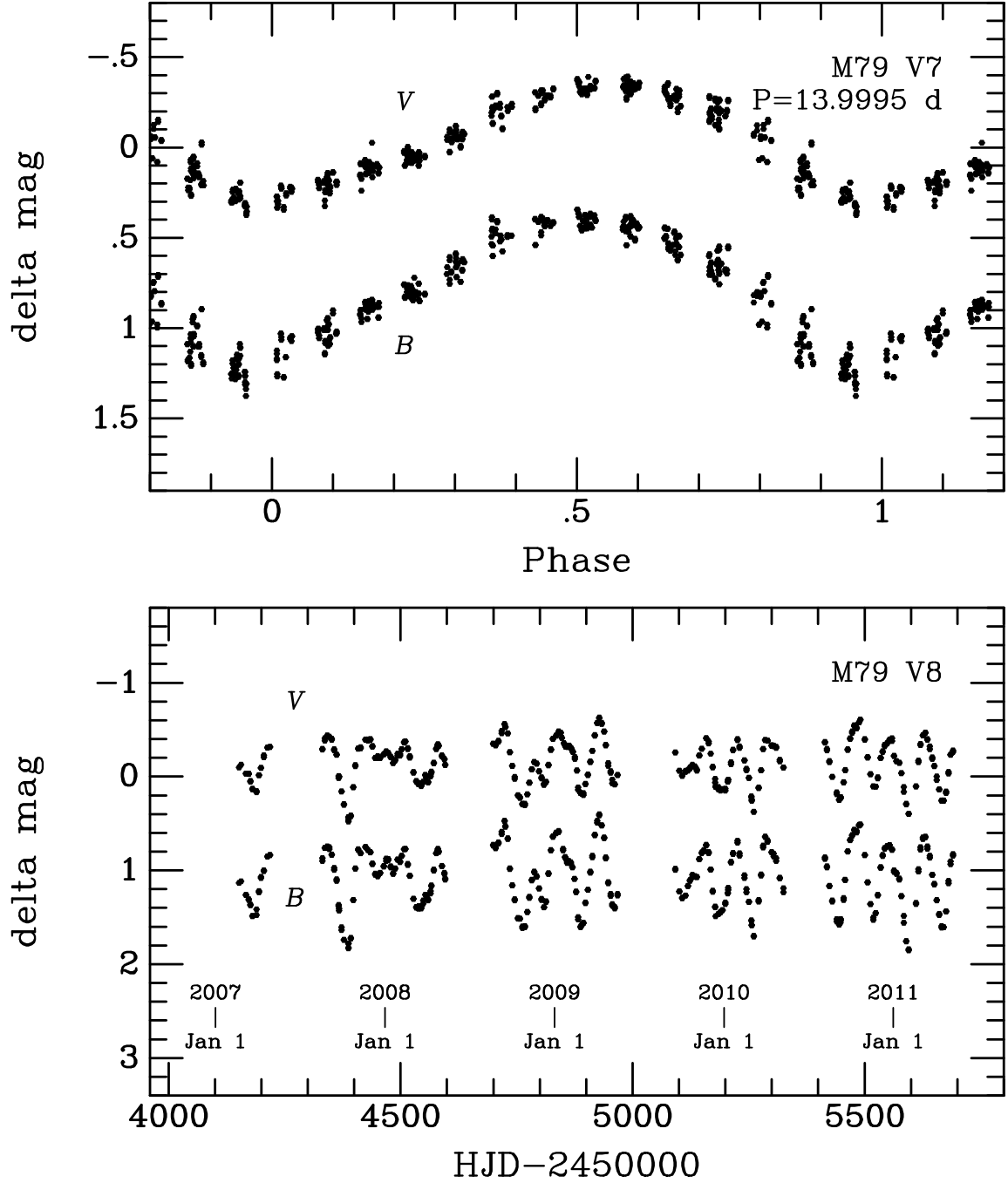


Fig. 9.— **Top:** Light curves of the W Virginis-type Cepheid M79-V7 in *V* and *B*, phased with a period of 13.9995 days. **Bottom:** Light curves of the semiregular variable M79-V8 in *V* and *B*. The characteristic pulsation period varies from about 65 to 80 days. In both plots, the magnitude zero-points are arbitrarily chosen.

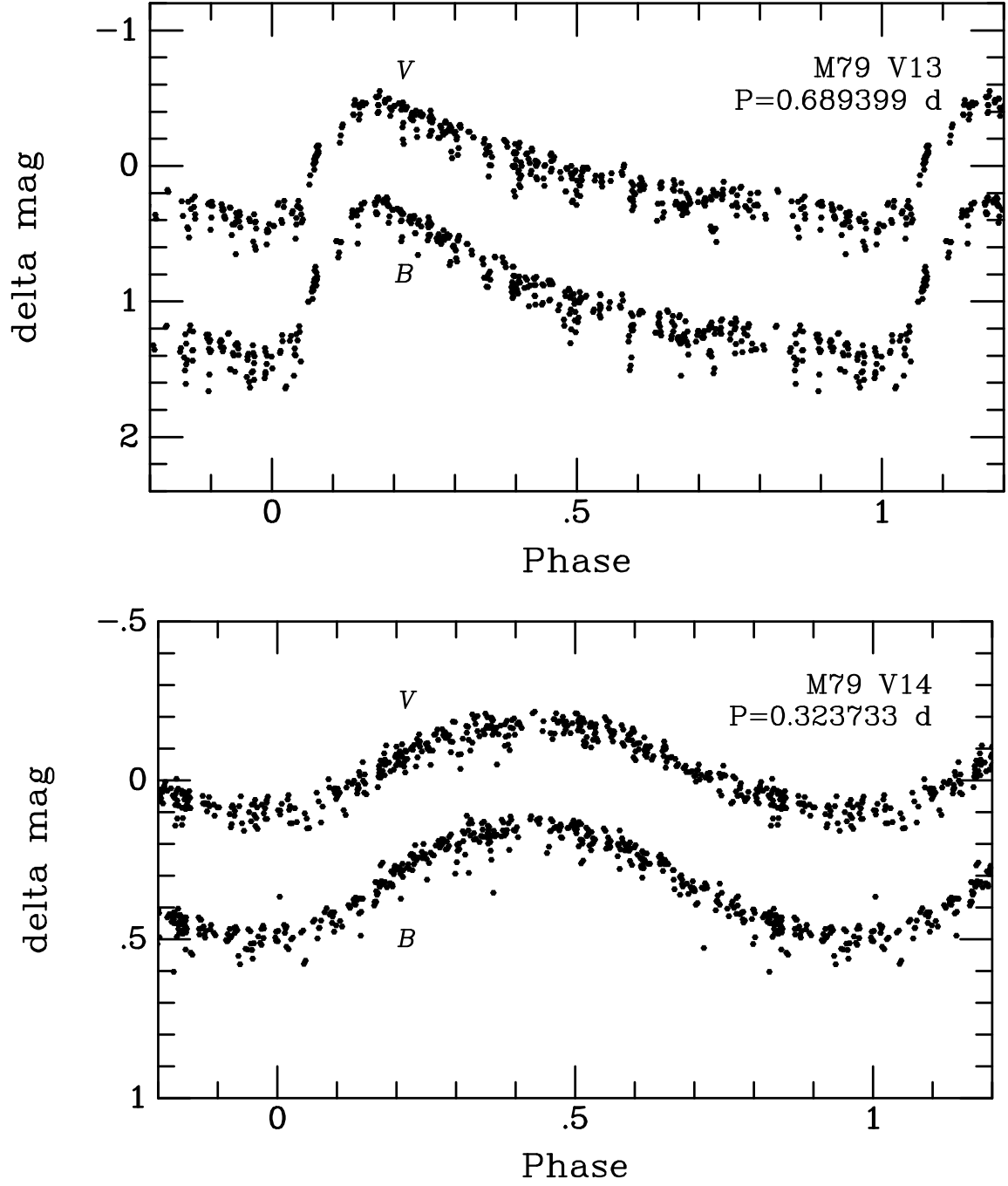


Fig. 10.— **Top:** Light curves of the RRab variable M79-V13 in V and B , phased according to the elements given in Table 3. **Bottom:** Light curves of the R R c variable M79-V14 in V and B , phased according to the elements given in Table 3.

Table 1. PAGB and AGB-M Stars in M79

Designation	RA (J2000)	Dec (J2000)	V	$B - V$	$V - I$	$(u - B) - (B - V)$
PAGB ^a	5:24:10.36	−24:29:20.6	12.203 ± 0.008	0.277 ± 0.013	0.460 ± 0.013	1.045 ± 0.018
AGBM 1	5:24:08.86	−24:32:00.1	16.234 ± 0.021	-0.046 ± 0.038	-0.031 ± 0.034	0.438 ± 0.051
AGBM 2	5:24:13.45	−24:32:20.7	15.827 ± 0.012	-0.048 ± 0.021	-0.124 ± 0.020	0.686 ± 0.030
UIT 1 ^b	5:24:11.93	−24:32:20.1	18.427 ± 0.030	-0.346 ± 0.039	-0.656 ± 0.141	-0.190 ± 0.051
UIT 2	5:24:12.69	−24:30:43.4	16.834 ± 0.020	-0.125 ± 0.031	-0.131 ± 0.052	0.206 ± 0.044

^aThe PAGB star is also cataloged as TYC 6479-422-1 and 2MASS J05241036−2429206.

^bUIT 1 is very faint in our frames, except in u , and the data are only approximate.

Table 2. Absolute Magnitudes of PAGB Candidates in Globular Clusters

Cluster	Star	Photometry			Distance	
		V	Source	$(m - M)_V$	Source	$M_{V,0}$
ω Cen	ROA 24	10.89	(1)	13.99	(4)	−3.10
NGC 5986	PAGB 1	12.65	(2)	16.05	(2)	−3.40
"	PAGB 2	12.76	"	"	"	−3.29
M79	PAGB	12.20	(3)	15.66	(5)	−3.46

References. — References for photometry of the PAGB stars and apparent V -band distance moduli of clusters are: (1) van Leeuwen et al. (2000); (2) Alves et al. (2001); (3) this paper; (4) Matsunaga et al. (2006); (5) Kains et al. (2012).

Table 3. M79 Variables in our 1.3-m Monitoring Field

Designation	Type	T_0 [HJD–2450000]	P [days]
V6	RRc	var. ^a	var. ^a
V7	CW	4139.450	13.9995
V8	SRd	...	65.1–80.1
V13	RRab	4151.442	0.689399
V14	RRc	4151.207	0.323733

^aSee Table 4 for seasonal elements.

Table 4. Elements for M79-V6

Season	T_0 [HJD–2450000]	P [days]
2007	4151.216	0.339122
2007–2008	4151.244	0.339076
2008–2009	4151.295	0.339036
2009–2010	4151.253	0.339051
2010–2011	4151.253	0.339145

Table 5. Differential Photometry of Variable Stars in M79^a

HJD–2450000	Delta Magnitude ^b
M79 V6 <i>B</i> Magnitudes	
4151.57438	3.7985
4156.58235	3.8212
4166.53713	3.4525
4166.53799	3.4358
4172.51951	3.8042

^aTable 5 is published in its entirety in the electronic edition of the journal. A portion is shown here for guidance regarding its form and content.

^bThe magnitudes are differential with respect to the sum of the intensities of eight comparison stars in the 1.3-m field.